Microelectrophoresis of a Bilayer-Coated Silica Bead in an Optical Trap: Application to Enzymology

R. Galneder,* V. Kahl,* A. Arbuzova,† M. Rebecchi,† J. O. Rädler,* and S. McLaughlin†
*Institut für Biophysik, Physik Department, Technische Universität München, 85747 Garching, Germany; and †Department of Physiology and Biophysics, State University of New York, Stony Brook, New York 11794 USA

ABSTRACT We describe an apparatus that combines microelectrophoresis and laser trap technologies to monitor the activity of phosphoinositide-specific phospholipase C-δ_1 (PLC-δ) on a single bilayer-coated silica bead with a time resolution of ~1 s. A 1-μm-diameter bead was coated with a phospholipid bilayer composed of electrically neutral phosphatidylcholine (PC) and negatively charged phosphatidylinositol 4,5-bisphosphate (2% PIP_2) and captured in a laser trap. When an AC field was applied (160 Hz, 20 V/cm), the electrophoretic force produced a displacement of the bead, Δx, from its equilibrium position in the trap; Δx, which was measured using a fast quadrant diode detector, is proportional to the zeta potential and thus to the number of PIP_2 molecules on the outer leaflet (initially, $\sim 10^5$). When a solution containing PLC-δ flows past the bead, the enzyme adsorbs to the surface and hydrolyzes PIP_2 to form the neutral lipid diacylglycerol. We observed a nonexponential decay of PIP_2 on the bead with time that is consistent with a model based on the known structural properties of PLC-δ.

GLOSSARY

a	constant
c	constant
e	electronic charge
E	electric field
E_0	electric field applied at the electrodes
f	frequency
f_c	corner frequency, Eq. 4
f_{ext}	frequency of the applied electric field
Δf	width of a frequency channel; $\Delta f = 1/t_{tot}$
F_{el}	electrophoretic force, Eq. 6
$F_{stoch}(t)$	random thermal force, Eq. 1
k	constant
k_B	Boltzmann constant
K	association constant
n	number of PIP_2 molecules on the outer leaflet of the coated bead
N	number of ions per unit volume in the bulk solution
P^V	plateau value of an uncalibrated voltage power spectrum, Eq. 5
r	radius of the bead
$S^V(f)$	voltage power spectrum
$S^x(f)$	displacement power spectrum of the bead in the trap, Eq. 3
[S]	substrate concentration
t	time
t_{tot}	total period of measuring time
T	temperature
v	velocity of the bead
x	distance
Δx	displacement of the bead from its equilibrium position, x_o, in the trap; $\Delta x = x - x_o$, Eq. 6
α	constant defined in Appendix II
β	detector sensitivity, Eq. 5
γ	Stokes drag coefficient for a sphere, Eq. 2
ϵ_r	dielectric constant of the solution
ϵ_o	permittivity of free space
ζ	zeta potential, Eq. 7
η	viscosity of the solution
κ	stiffness of the trap, Eq. 1
λ	Debye length
σ	fixed charge density (charge/area on the outer leaflet of a coated bead)

Received for publication 3 October 2000 and in final form 10 December 2001.

Address reprint requests to Dr. Stuart G. McLaughlin, SUNY Health Science Center, Department of Physiology/Biophysics, Stony Brook, NY 11794-8661. Tel.: 631-444-3615; Fax: 631-444-3432; E-mail: smcl@epo.som.sunysb.edu.

0006-3495/01/05/2298/12 $2.00

INTRODUCTION

We have constructed an apparatus that is capable of rapidly and accurately monitoring the activity of enzymes that modify the charge of their membrane-bound substrates and used it to study the well-characterized enzyme phosphoinositide-specific phospholipase C-δ_1 (PLC- δ). As shown in Fig. 1 *A*, we used a focused laser beam to trap a small silica bead coated with a phospholipid bilayer. The bilayer coating the bead comprises a mixture of the zwitterionic lipid phosphatidylcholine (PC) and the negatively charged lipid phosphatidylinositol 4,5-bisphosphate (PIP_2), which is the membrane-bound substrate of PLC-δ. Application of an electric field exerts an electrophoretic force, F_{el}, that produces a displacement of the bead, Δx, from its equilibrium position in the trap. By calibrating the trap and determining its stiffness, or spring constant, κ, we can calculate the electrophoretic force exerted on the coated bead by the field, $F_{el} = \kappa \Delta x$. Control experiments show, as predicted theoretically, that F_{el} is proportional both to the applied electric field and to the zeta potential, the electrostatic potential at the shear plane adjacent to the coated bead. To a good approximation, the zeta potential is proportional to the number of fixed negative charges (PIP_2) on the outer leaflet of the coated bead (initially $n \approx 10^5$).

Fig. 1 *B* shows a small portion of a bilayer-coated silica bead with a single adsorbed PLC-δ. PLC-δ adsorbs to the membrane mainly because of a high-affinity association of its pleckstrin homology (PH) domain with PIP_2 (see Appendix I). The active site in the catalytic domain of a membrane-bound PLC-δ then hydrolyzes PIP_2. As shown schematically in Fig. 1 *B*, this hydrolysis produces two

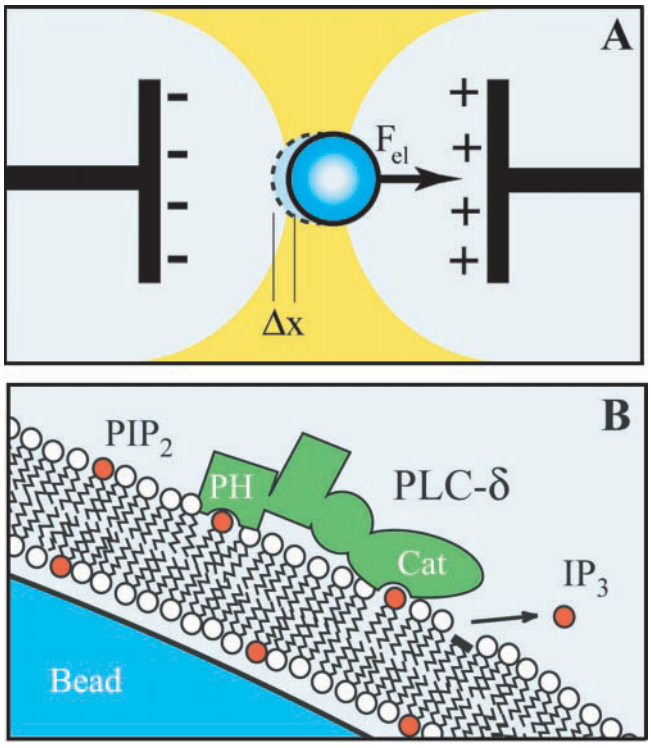

FIGURE 1 Principle of operation of the field/trap apparatus. (*A*) Sketch of a bilayer-coated silica bead (blue sphere) in a laser trap (yellow) exposed to an electric field. Applying an electric field via the electrodes (black rectangles with + and − signs) produces an electrophoretic force (F_{el}) on the bead due to the fixed negative charges (PIP_2) on the outer leaflet of the bilayer. This force causes a displacement (Δx = 10–100 nm) of the bead from its equilibrium position in the tightly focused laser beam. (*B*) Sketch of a small portion of the 500-nm-radius silica bead (blue) coated with a phospholipid bilayer consisting of 98% PC (zwitterionic lipids with white polar headgroups) and 2% PIP_2 (acidic lipids with red headgroups). The bilayer thickness is ~5 nm, and the adsorbed PLC-δ_1 enzyme (green) is drawn to scale from the known structures of the PH domain and the remainder of the molecule, which contains a catalytic (Cat) domain. The hydrolysis of negatively charged PIP_2 produces electrically neutral diacylglycerol (decapitated lipid below *arrow*), which remains in the membrane. The negatively charged headgroup, inositol 1,4,5-trisphosphate (IP_3; red circle in aqueous phase), diffuses away from the bead.

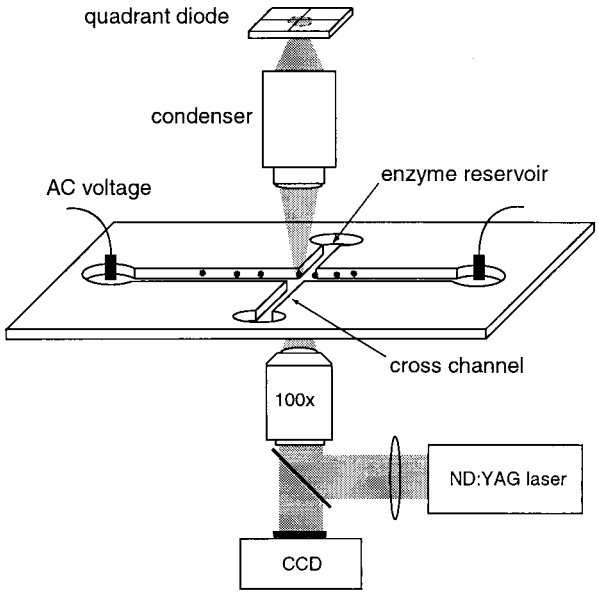

FIGURE 2 Sketch of the field trap apparatus. See text for details.

biologically important second messengers: the electrically neutral lipid diacylglycerol remains in the membrane, and the negatively charged headgroup (inositol 1,4,5-trisphosphate (IP_3)) diffuses away from the bead. Thus hydrolysis of PIP_2 by PLC-δ reduces the charge on the outer leaflet of the coated bead and, concomitantly, its displacement in the applied field. We monitor the number of PIP_2 molecules on the bead as a function of time after exposure to PLC-δ by measuring Δx.

Fig. 2 illustrates the apparatus we constructed to make these measurements. As described in more detail in Materials and Methods, we used a tightly focused beam of light from a Nd:YAG laser to trap a bilayer-coated silica bead (filled circle) at the intersection of the main and cross-channels in the chamber. The image of the trapped bead is projected onto a fast quadrant diode, which monitors the motion of the bead. Analysis of the Brownian motion of the bead allows us to determine both the sensitivity of the detector (voltage output/displacement) and the stiffness of the laser trap (displacement/force). The theoretical and experimental aspects of constructing a trap suitable for use with a small silica bead have been considered in authoritative reviews (e.g., Ashkin, 1997; Svoboda and Block, 1994) and monographs (e.g., Sheetz, 1998); the use of a quadrant diode to monitor the motion of the bead is discussed by Mehta et al. (1998); and analysis of the power spectrum of the Brownian motion of a small bead in a laser trap is treated in a clear, pithy manner elsewhere (Gittes and Schmidt, 1998; Svoboda and Block, 1994).

Applying an AC voltage through the electrodes produces an electrophoretic force (F_{el} in Fig. 1 *A*) that displaces the bead; we monitor the displacement, Δx, by analyzing the power spectrum as we discuss in Materials and Methods. When we open the valves on the cross-channel and apply a pressure gradient to the fluid in it, PLC-δ flows from the enzyme reservoir past the coated bead in the trap (Fig. 2). The enzyme binds to the coated bead and hydrolyzes PIP_2, reducing the net charge on the outer leaflet of the bilayer (Fig. 1 *B*) and, thus, the displacement that we measure. Several design aspects of the chamber shown in Fig. 2 were crucial for the success of the field/trap experiment, and these are described in some detail in Materials and Methods because we know of no other work in which microelectrophoresis and optical tweezers were used to measure enzyme activity.

The experiment we describe is similar in principle to the classical Millikan oil drop experiment. Millikan (1917) bal-

anced the gravitational force on a charged oil droplet with an opposing electrical force. The method was sufficiently sensitive to measure accurately the charge of a single electron adsorbed to the oil droplet. In our case, a focused beam of laser light rather than gravity exerts the non-electrical force on the bead. A more important difference is that our coated bead is in an electrolyte solution, whereas Millikan's oil droplet was suspended in air between two capacitor plates. Application of an electric field not only exerts a direct electrical force on the coated bead due to the fixed negative charges (PIP_2) on the outer leaflet, but also induces a flow of fluid adjacent to the bead that produces an opposing force (electrophoretic retardation). The fluid flow occurs because the applied field exerts a force on the counterions in the diffuse double layer (thickness of ion atmosphere $\approx$ Debye length, λ), which is transferred to the adjacent fluid. The physics describing the electrophoresis of a large (radius $\gg \lambda$) sphere is well understood (e.g., Overbeek and Wiersema, 1967; Hunter, 1981); Helmholtz and Smoluchowski made major contributions to our understanding of electrokinetic phenomena a century ago. We use the Helmholtz-Smoluchowski equation, which gives the proportionality constant between the steady-state velocity of a free charged particle and the magnitude of the applied electric field, together with the Stokes relation (see below) to express the net electrophoretic force exerted by the applied electric field on the coated bead in our laser trap.

We chose PLC-δ for our initial studies with the field/trap apparatus for three primary reasons. First, the enzyme is important biologically; it cleaves PIP_2 to produce two second messengers, diacylglycerol and inositol 1,4,5-trisphosphate, which contribute to protein kinase C activation by different mechanisms (see, e.g., Berridge, 1993; Clapham, 1995; Hurley and Grobler, 1997; Newton, 2000; Hurley and Misra, 2000; Rhee et al., 2000). Second, the structure of the enzyme is known. PLC-δ comprises, in sequence from the N terminus, PH, EF hand, catalytic, and C2 domains. The structures of the PH domain complexed with IP_3 (Ferguson et al., 1995) and the remainder of the enzyme (Essen et al., 1996; Grobler et al., 1996) have been determined by crystallography; the structure of the region linking the PH domain to the remainder of the molecule is unknown. Tracings of the PH domain and remainder of the molecule are juxtaposed in Fig. 1 *B* to illustrate the size of the enzyme relative to the bilayer. Third, the molecular mechanism by which the enzyme hydrolyzes PIP_2 is well understood (Hondal et al., 1998, and references therein). PLC-δ catalyzes hydrolysis of the O-P bond connecting inositol to diacylglycerol. The PLC-δ_1 active site is a shallow cavity located at one end of the catalytic barrel (Essen et al., 1996). Substrate binds to the active site through a network of hydrogen bonds and salt-bridges that ligate the inositol ring substituents, explaining the preference for $PI(4,5)P_2$. An essential calcium ion also binds to the active site and is thought to both lower the pKa of the attacking hydroxyl and disperse the negative charge of the transition state (Essen et al., 1997).

In contrast to our detailed understanding of the structure and function of PLC-δ, we know relatively little about its behavior on membrane surfaces. Previous work employed phospholipid vesicles containing PIP_2 to study PLC-catalyzed reactions, but the progress curves (percent PIP_2 hydrolyzed versus time) are difficult to interpret because of two factors that can limit the reaction rate: the exchange of enzyme between surfaces and inhibition by the IP_3 product. The field/trap apparatus we describe eliminates these complications. First, measurements are made on a single coated bead, so there is no problem with exchange of PLC-δ between different surfaces. Second, the flow of fluid past the bead rapidly sweeps the IP_3 product away from the bead surface, so it does not inhibit the enzyme. The time for diffusion through the unstirred layer (thickness $\approx$ radius of bead) adjacent to the bead is negligible ($\sim$1 ms), and measurements can be made rapidly (initial mixing time and time resolution $\approx$ 1 s). We compare the progress curves obtained using the field/trap approach with the predictions of a simple kinetic model and then discuss how the field trap apparatus might be used to study the activity of single molecules of PLC-δ and other enzymes that modify the surface charge of phospholipid bilayers.

MATERIALS AND METHODS

Preparation of bilayer-coated silica beads

Silica beads (0.99 $\pm$ 0.05 μm diameter, 2% solids; Duke Scientific, Palo Alto, CA) were bath sonicated in methanol, centrifuged, resuspended in 1 N KOH, bath sonicated again, and then washed more than five times in deionized water. Palmitoyloleoyl-phosphatidylcholine (PC, 25 mg/ml in chloroform; Avanti Polar Lipids, Alabaster, AL) was mixed with 2 mol % of the ammonium salt of phosphatidylinositol 4,5-bisphosphate (PIP_2, 4 mg/ml in chloroform; purified as described in Morris et al., 1995) and an extra 0.6 ml of chloroform in a 50-ml round-bottom flask. (It is important to use the ammonium salt of PIP_2; the sodium salt is less soluble in chloroform, does not form a uniform film with PC when dried, and results in a nonuniform distribution of PIP_2 between PC/PIP_2 vesicles when the film is hydrated (Toner et al., 1988).) The solution was dried rapidly in a rotary evaporator under vacuum ($\sim$100 mbar) maintaining the flask at $\sim$30°C in a water bath, which allows formation of a uniform lipid film and prevents the lipids from phase separating during removal of the solvent. We removed all traces of the chloroform solvent, which can catalyze breakdown of lipids during sonication, by maintaining a hard vacuum ($\sim$10 mbar) for at least 2 h. We formed multilamellar vesicles by adding 2.5 ml of water and swirling the flask and then sonicated the suspension to clarity with a tip sonicator. The sonication step, which required $\sim$10–20 min, was performed with the vessel in a 10°C water bath using sonication cycles of 10 s on followed by 30 s off to minimize local overheating and concomitant breakdown of PIP_2, which is more sensitive to breakdown under sonication than most lipids. The sonicated unilamellar vesicles (SUVs) were separated from any residual multilamellar vesicles and titanium fragments by ultracentrifugation at $\sim$100,000 $\times$ *g* for 30 min (Barenholz et al., 1977), and the upper two-thirds of the supernatant was retained. An excess of freshly prepared SUVs was mixed with freshly washed silica beads in water, and 1–2 μM $CaCl_2$ was added to promote fusion of the vesicles onto the beads. Beads were allowed to sediment, a process that required several hours, and

the supernatant was replaced by a solution containing 10 mM HEPES, 300 μM EGTA, 200 μM $CaCl_2$ (free $Ca^{2+} \approx 0.5$ μM as measured directly with an electrode), pH 7.0. The ionic strength of the final solution was ~3.5 mM, producing a Debye length of $\lambda \approx 5$ nm.

Flow chamber

The chamber is designed as a sandwich assembly consisting of (from bottom to top) a glass coverslip (60 × 24 mm), thermoplastic foil (Xiro, Schmitten, Switzerland), a microscope glass slide (60 × 24 mm) with four holes to access the channels, and a polycarbonate supporting block (90 × 26 mm). Cuts in the thermoplastic foil form the rectangular cross-channel system between the two glass slides; each channel is 1.5 mm wide and ~90 μm high. The main channel (48 mm long) has platinum black electrodes connected at both ends and is used for electrophoresis. The cross-channel, which was ~14 mm long and perpendicular to the main channel (Fig. 2), was used to inject the PLC-δ solution. Liquid flows in only one channel at a time; flow is controlled by varying the hydrostatic pressure independently using micrometer screws to adjust the heights of the hydrostatic pressure reservoirs. The reservoirs are connected with the chamber via Teflon (PTFE) tubing and Teflon valves; control measurements showed that PLC-δ does not adsorb significantly to PTFE tubing. We preloaded PLC-δ (1–10 nM) in a PTFE tubing loop before it was connected to the side port, flushed the system with the PLC-δ solution to minimize the dead time (time required for the concentration of PLC-δ in the solution flowing past bead to increase to 90% of its final value; ~1 s), and then washed the PLC-δ out of the intersection by flowing fluid through the main channel. This flow continued until a bead was trapped, and then all flow was stopped. After initial measurements of the zeta potential of the bead, the side port was opened and the PLC-δ solution flowed past the bead.

We minimized loss of enzyme during the experiment by coating the entire inside glass surface of the measuring chamber with a bilayer of PC before each day's experiments; PLC-δ binds strongly to glass but does not bind significantly to PC bilayers (Rebecchi et al., 1992). Coating the chamber with electrically neutral PC also minimizes electro-osmosis, the field-induced flow of fluid adjacent to a charged surface (Hunter, 1981). Coating involved injecting SUVs composed of PC plus 0.1% NBD-PC in 50 mM NaCl, 5 mM Tris, pH 8 (Groves and Boxer, 1995; Groves et al., 1998) and then removing excess vesicles by extensive rinsing with water. (The PC-coated chamber was typically used for one day's experiments. The glass chamber can be reused if it is cleaned with a detergent solution and then washed extensively with water before applying a fresh PC coat.) The quality of the PC coating was checked optically by fluorescence microscopy and indirectly by measuring the apparent electrophoretic mobility of electrically neutral PC multilamellar vesicles under low-salt conditions. When the coating was satisfactory, the velocity of the PC vesicles in an applied DC electric field was zero at all distances from the surface. We minimized any possible effects of electro-osmosis by trapping a bead ~20 μm from the surface, the location of stationary layer for this rectangular chamber (Hunter, 1981). This distance also is far enough from the surface to render hydrodynamic drag effects unimportant (Faxen's law), as discussed elsewhere (Svoboda and Block, 1994).

Experimental protocol

In a typical experiment (e.g., Fig. 6), we used hydrostatic pressure to flow coated beads into the main channel while the cross-channel, which had been preloaded with the PLC-δ solution, remained closed. The focused laser beam at the intersection of the two channels trapped a coated bead (Fig. 2), and we determined the zeta potential by applying a 160-Hz AC field, as described below. We monitored the zeta potential with the AC field for ~100 s to ensure it was constant and then closed the main channel and flowed the PLC-δ into the side channel at a constant rate. The cross-channel solution contained 10 mM HEPES, 300 μM EGTA, 200 μM $CaCl_2$, free $[Ca^{2+}] \approx 0.5$ μM, 2 mM dithiothreitol, pH 7, and typically either 0, 1, 3, or 9 nM PLC.

Phosphoinositide-specific phospholipase C-δ_1

Human PLC-δ was expressed in BL-21(DE3) strain of *Escherichia coli* using the pET3a vector as described previously (Tall et al., 1997). PLC-δ activity was monitored during purification using a detergent/PIP_2 mixed-micelle assay (Cifuentes et al., 1993). We calculated the PLC-δ concentration based on absorption at 280 nm using a molar extinction coefficient of 116,000 M^{-1} cm^{-1} (Tall et al., 1997).

Instrumentation

As illustrated in Fig. 2, a 300-mW diode-pumped Nd:YAG laser (Coherent, Lübeck, Germany) was steered into an axiovert 135 TV Zeiss microscope outfitted with an oil-immersion objective (Plan-Neofluoar, 100×, 1.3 NA; Carl Zeiss, Oberkochen, Germany). The laser beam was refocused by a condenser and imaged on a Hamamatsu quadrant diode S5981 (Hamamatsu City, Japan) to measure the position of the bead. The electronic bandwidths of both the quadrant diode and the current-voltage converter are >70 kHz. The amplified signal from the diode was digitized at 16 kHz (National Instruments PCI-Mio-16E4, Austin, TX), fast Fourier transforms of the signal were computed continuously at 1-s intervals for time sequences of 500 ms (8192 data points), and the corresponding power spectra were saved.

Power spectrum analysis

As described in standard reviews (e.g., Gittes and Schmidt, 1998), the voltage power spectrum $S^V(f)$ measured with the quadrant diode is proportional to the displacement power spectrum of the bead in the trap: $S^V(f) = \beta^2 S^x(f)$, where β is termed the detector sensitivity, f is frequency, and x is distance. We calibrated the trap by obtaining values for both the detector sensitivity, β, and the trap stiffness, κ, the proportionality constant that relates the displacement of the trapped bead from its equilibrium position (in Fig. 1, $\Delta x = x - x_0$, where x_0 is the equilibrium position) to the electrophoretic force, $F_{el} = \kappa \Delta x$. We did this by analyzing the power spectrum due to the Brownian motion of the bead without an external AC field. As discussed elsewhere, the Brownian motion of a bead near the center of an optical trap is described by the Langevin equation (e.g., Svoboda and Block, 1994; Gittes and Schmidt, 1998):

$$\kappa \Delta x + \gamma \frac{dx}{dt} = F_{stoch}(t), \tag{1}$$

where $F_{stoch(t)}$ is the random thermal force and

$$\gamma = 6\pi\eta r \tag{2}$$

denotes the Stokes drag coefficient for a sphere of radius r moving in a fluid with viscosity η. As illustrated in Fig. 3 *A*, the corresponding power spectrum is of Lorentzian form:

$$S^x(f) = \frac{k_B T}{\gamma \pi^2 (f_c^2 + f^2)}, \tag{3}$$

where k_B is the Boltzmann constant, T is the temperature, and

$$f_c = \frac{\kappa}{2\pi\gamma} \tag{4}$$

is the corner frequency. The corner frequency divides the Brownian motion into two regions. When $f \ll f_c$, the power spectrum is constant and the

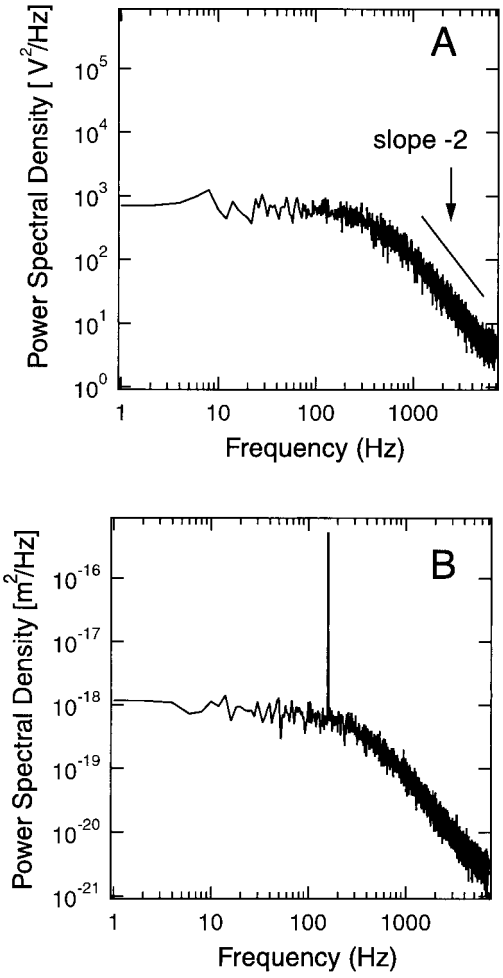

FIGURE 3 Calibration of the laser trap. (*A*) A typical power spectrum (average of 20 0.5-s spectra) due to the Brownian motion of a 500-nm-radius bead in the laser trap. The power spectral density is obtained from the voltage output of the quadrant diode illustrated in Fig. 2. As described in the text, analysis of a power spectrum allows us to obtain values for both the detector sensitivity, β, and the trap stiffness, κ. (*B*) Determination of zeta potential. Applying a 160-Hz AC field to a coated bead in the calibrated laser trap produces this typical displacement power spectrum. The field-induced oscillation of the bead in the trap manifests itself as the peak in the power spectrum at 160 Hz. As we discuss in the text, the square root of the peak height is proportional to the zeta potential and, thus, the number of PIP_2 molecules on the bead. This figure depicts the average of 15 spectra, but we typically averaged only 3 spectra to improve the time resolution of our on-line measurement of the zeta potential (e.g., Fig. 6 *C*). The beads used to generate the data in Figs. 3, 4, 6, 7, and 8 were coated with a PC/PIP_2 bilayer (2% PIP_2) and suspended in a solution containing 10 mM HEPES, pH 7.0, 300 μM EGTA, 200 μM calcium, ~0.5 μM free Ca^{2+}.

silica bead experiences the confining force of the trap. When $f \gg f_c$, the power spectrum decays as $1/f^2$, as is the case for free diffusion; at these short times the silica bead does not experience the confining force of the trap. The spectrum shown in Fig. 3 *A* is similar to those reported in the literature (e.g., Fig. 4 of Gittes and Schmidt, 1998).

We determined the value of β, the detector sensitivity, from an uncalibrated voltage power spectrum, such as the one illustrated in Fig. 3 *A*, by multiplying the spectrum by f^2 and noting the plateau value, P^V, for $f \gg f_c$. As described elsewhere (Allersma et al., 1998),

$$\beta^2 = \frac{P^V \pi^2 \gamma}{k_B T}. \tag{5}$$

We determined the corner frequency from a least-squares fit of the power spectrum data, such as shown in Fig. 3 *A*, with a Lorentzian function. The stiffness of the trap, κ, was then determined directly from Eq. 4 (Florin et al., 1998) using the measured value of the corner frequency and value of the Stokes drag coefficient, γ, calculated from Eq. 2 using the known radius of the bead (r = 500 nm).

Once the trap was calibrated, we could measure the displacement of the bead produced by application of a known electric field. Application of an AC field (maximum field, E_0 = 100 V/4.8 cm; f_{ext} = 160 Hz) causes the charged bilayer-coated bead to oscillate in the trap. (Theory predicts and experiments confirm that neither the charge on the inner leaflet nor the silica bead has a significant effect on the zeta potential; only the charges on the outer leaflet sense the applied potential. This follows because the capacitance of the membrane is only ~2% of the capacitance of the diffuse double layer.) The oscillation manifests itself as a peak in the displacement power spectrum shown in Fig. 3 *B* at the applied frequency f_{ext}. The peak height in Fig. 3 *B* is proportional to the square of the maximum displacement of the bead in the trap. The potential near the center of an optical trap is harmonic, so the displacement of the bead in the trap, Δx, is proportional to the applied electrophoretic force (F_{el} in Fig. 1) divided by the product of the trap stiffness, κ, and a damping factor (Svoboda and Block, 1994)

$$\Delta x = \frac{F_{el}}{\kappa(1 + f_{ext}^2/f_c^2)^{1/2}}. \tag{6}$$

For the bilayer-coated silica bead illustrated in Fig. 3 *B*, the corner frequency is 350 Hz, and the frequency of the applied field is 160 Hz; the damping factor represents only a 10% effect.

When an electric field, E, is applied to either a phospholipid vesicle or a bilayer-coated silica bead, the Helmholtz-Smoluchowski equation relates the steady-state velocity, v, to the zeta potential, ζ, the potential at the hydrodynamic plane of shear, which is ~0.2 nm from the surface of a bilayer (McLaughlin, 1989):

$$\zeta = \frac{v\eta}{\epsilon_r \epsilon_o E}, \tag{7}$$

where η is the viscosity of the solution, ϵ_r is the dielectric constant, and ϵ_o is the permittivitiy of free space. Eq. 7 is derived in standard sources (e.g., Overbeek and Wiersema, 1967) and is valid when relaxation effects are negligible; relaxation effects arise because the applied electric field perturbs the spherical diffuse double layer of counterions around the negatively charged coated bead. Theory predicts relaxation effects are negligible for our experimental conditions because the radius of the bead (r = 500 nm) is much larger than the thickness of the double layer (Debye length $\lambda \approx 5$ nm) and the zeta potential ($\zeta \approx -50$ mV) is not too high (e.g., O'Brien and White, 1978; Hunter, 1981). Experiments confirm relaxation effects are indeed negligible for our experimental conditions; specifically, ζ does not change as the radius of multilamellar vesicles increases to values 10-fold greater than the radius of the coated beads (data not shown).

Although we use Eq. 7 to calculate ζ for a coated bead by measuring its velocity in a DC field with the laser trap off (see below), we are mainly interested in the electrophoretic force exerted on the coated bead by the electric field, F_{el}, when the bead is in the laser trap. (We ignore the fact we are applying an AC field with a frequency < 1 kHz, because the time for a micrometer-size sphere to accelerate to its final velocity is <1 μs (e.g., see p. 77 of Berg, 1983). O'Brien and White (1978) provide the required solution. Noting that the differential equations required to describe the electrophoretic mobility of a particle are linear, they decomposed the

problem of describing the mobility into two simpler problems. First, they calculate the force required to move the particle at a constant velocity with no applied field. Second, they calculate the force required to hold the particle fixed in the presence of an applied field, which by definition is F_{el} in our field trap experiment. The total force acting on a particle is the sum of these two forces, which is zero for a particle moving with a constant velocity. The first force is the hydrodynamic drag, which is the Stoke's drag given by Eq. 2, $6\pi\eta rv$, for our spherical coated bead. For the free particle, we have $F_{el} = 6\pi\eta rv$; combining this equation with Eq. 7 we obtain the following relation between F_{el} and the zeta potential:

$$\zeta = \frac{F_{el}}{6\pi r\epsilon_r\epsilon_o E}. \tag{8}$$

Thus, by continuously measuring the peak amplitude at f_{ext} in the sequence of power spectra produced (e.g., Fig. 3 *B*), it was possible to monitor the zeta potential online. As we discuss below (see Eq. 9), the zeta potential is, to a first approximation, proportional to the charge density of the bilayer-coated bead. Thus, the initial zeta potential of −55 mV corresponds to the 90,000 PIP_2 molecules present on the coated bead before the addition of PLC, and the decay of the zeta potential we observe with time (e.g., Fig. 6 *C*) reflects a proportional decay in the number of PIP_2 molecules on the bead.

Experimental tests of the calibration procedure

Before and at the end of each experiment we determined the zeta potential in the conventional manner by measuring the velocity of the coated bead in a known DC electric field. Specifically, we released the laser trap, visualized the bead on a screen with the CCD camera shown in Fig. 2, applied a DC field (typically 2 V/cm) for 5 s, and measured the distance the coated bead moved in this time (typically, ~50 μm before addition of PLC). We then reversed the field and measured the distance moved by the bead in the reverse direction, whereupon the bead was again trapped and the experiment continued. We always observed an agreement (within the experimental 5% accuracy of the DC measurements) between the zeta potential measured in the conventional way and the zeta potential measured using the field/trap apparatus. This controls for several potential artifacts that could have arisen during the field/trap experiment.

The combination of Eqs. 6 and 8 predicts that the displacement of the bead in the trap varies linearly with the applied electric field. (In other words, the stiffness of the trap should be a constant.) Fig. 4 illustrates that there is indeed an excellent linear relationship between the magnitude of the applied field (the applied voltage drops over the 4.8-cm length of our chamber) and the amplitude of the bead vibration (<30 nm) measured using data such as those illustrated in Fig. 3 *B*. This result is consistent with reports from other laboratories. Using similar conditions (600-nm-diameter bead; f_c = 544 Hz), Svoboda and Block (1994) noted that the stiffness was constant out to 150 nm, beyond which it decreased. The typical correlation coefficient for the displacement/voltage curves (e.g., Fig. 4) was >0.99.

Under our conditions, ζ is approximately proportional to the number of negatively charged PIP_2 molecules on the outer leaflet of the coated bead. Gouy-Chapman theory suggests and experiments confirm (e.g., McLaughlin, 1989) that the zeta potential (which is approximately equal to the surface potential under our conditions) is

$$\sinh(e\zeta/2k_BT) = \sigma/(8N\epsilon_r\epsilon_o k_BT)^{1/2}, \tag{9}$$

where e is the electronic charge, σ is the fixed charge density (charge/area on outer leaflet), and N is the number of ions per unit volume in the bulk solution. To the extent that $\sinh x = x$ is a valid approximation, Eq. 9 predicts the zeta potential of the coated beads is proportional to the number of PIP_2 molecules per unit area in the outer leaflet. The points at the left of Fig. 5 show that under our experimental conditions (mole fraction of PIP_2 ≤ 2%) the zeta potential of a multilamellar PC/PIP_2 vesicle or coated bead

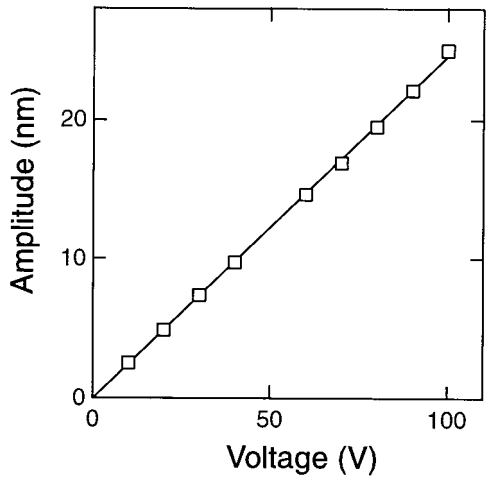

FIGURE 4 The amplitude of the voltage-induced displacement of a bilayer coated silica bead versus applied voltage. We used data averaged from 15 power spectra, as illustrated in Fig. 3 *B*, to obtain the displacement, which is proportional to the applied voltage (correlation coefficient > 0.99). The size of the square symbols is equal to the average SD of 10 measurements. We estimate we can deduce the displacement (or zeta potential) to an accuracy of ~1–2% by applying a voltage of 100 V to our coated beads and averaging 3 power spectra, a process that takes ~3 s.

(data not shown) is approximately proportional to the mole fraction of PIP_2.

As a control, we compared the zeta potential of multilamellar PC/PIP_2 vesicles containing 2% PIP_2 (Fig. 5) measured in a conventional DC microelectrophoresis apparatus designed by Bangham et al. (1958) with the zeta potential of the coated beads measured in the field trap apparatus (Fig. 6 *C* or Fig. 7). Finally, we note $[Ca^{2+}] > 1$ μM decreases the magnitude of the zeta potential (Fig. 5); thus, we used a free calcium concentration of ~0.5 μM for our experiments. Calcium ion concentrations > 2 μM also cause irreversible aggregation of the coated beads in our 10 mM HEPES solution (not shown); presumably calcium ions can chelate PIP_2 lipids on adjacent bilayers.

Detection limit of the field/trap apparatus

The detection limit of the field/trap apparatus is reached when the electrophoretic displacement (i.e., the peak observed at 160 Hz in Fig. 3 *B*) becomes lost in the Brownian noise. For a discrete power spectrum, the width of a frequency channel $\Delta f = 1/t_{tot}$, where t_{tot} denotes the total measurement period. The mean square deviation of fluctuations at a given frequency is $\langle x^2\rangle_{f=fo} = S^x(f = f_o)\Delta f$ (e.g., Svoboda and Block, 1994). Hence the minimum detectable electrophoretic force occurs when $\Delta x_{el} = (\langle x^2\rangle_{fo})^{1/2}$. Using Eqs. 3, 4, and 6, we obtain

$$F_{el}^{min} = (4k_BT\gamma\Delta f)^{1/2}. \tag{10}$$

From Eq. 8 we have that the minimum zeta potential:

$$\zeta_{min} = \frac{1}{\epsilon_r\epsilon_o E}\left(\frac{2k_BT\eta}{3\pi rt_{tot}}\right)^{1/2}. \tag{11}$$

For our system, η = 0.001 kg/(m s), $k_BT = 300 \times 1.3 \times 10^{-23}$ J, $\epsilon_r\,\epsilon_o = 80 \times 8.85 \times 10^{-12}$ C^2/(Jm), E = 100 V/5 cm = 2000 V/m, $r = 0.5 \times 10^{-6}$ m, and t_{tot} = 0.5 s, giving a minimum zeta potential ≈ 1 mV discernable above the noise level. This analysis agrees well with an inspection of Fig.

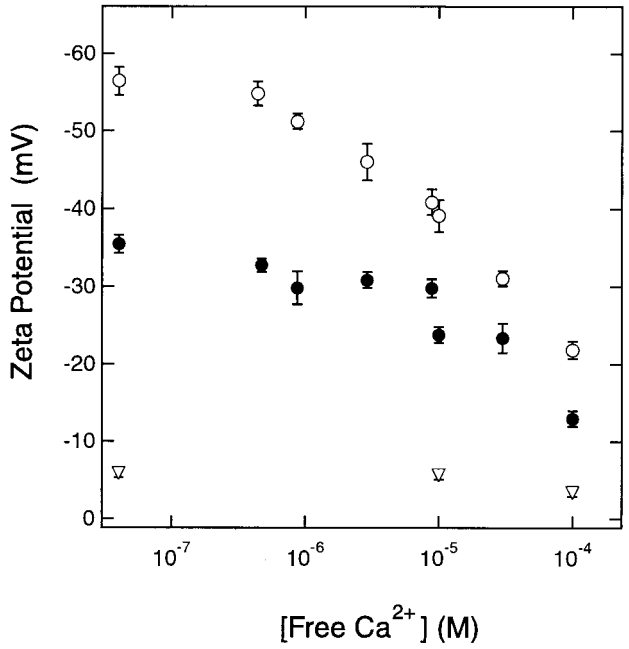

FIGURE 5 Effect of calcium ions on the zeta potential of PC/PIP_2 multilamellar vesicles. These measurements were conducted in a conventional DC microelectrophoresis apparatus described by Bangham et al. (1958). The three data points at the left of the graph (free $[Ca^{2+}] < 10^{-7}$ M) demonstrate that the zeta potential of a PC/PIP_2 vesicle depends, to a first approximation, linearly on the mole fraction of PIP_2 in the vesicle over the range 0–2% PIP_2. The relationship is given more exactly by the Gouy equation, Eq. 9. ▽, ●, and ○, measurements with vesicles formed from PC, PC/PIP_2 with 1% PIP_2, and PC/PIP_2 with 2% PIP_2, respectively. The figure also illustrates that free $[Ca^{2+}] > 1$ μM significantly deceases the zeta potential of the PC/PIP_2 (2% PIP_2) vesicles by binding to PIP_2. The aqueous solutions contained 10 mM HEPES (ionic strength ~3 mM), pH 7.0, 150 μM EGTA, at 25°C, and Ca^{2+} to bring the free $[Ca^{2+}]$ to the indicated value, as measured directly by a calcium electrode.

3 *B*: the peak at 160 Hz rises ~10^3-fold above the background, and the zeta potential (−55 mV) is proportional to the square root of this peak, suggesting we should be able to detect a potential of ~55/$(1000)^{1/2}$ or ~2 mV. This corresponds to ~2000 PIP_2 molecules. In some cases (low PLC concentration) we followed the change in zeta potential for ~1 h. In control experiments we found that the setup was stable within 3 mV over 1 h.

RESULTS

Monitoring the activity of PLC-δ enzymes with field/trap apparatus

Fig. 6 illustrates the first biophysical application of laser-trap-based microelectrophoresis: the field/trap apparatus can accurately record the hydrolysis of PIP_2 by a few membrane-bound PLC-δ enzymes (~100 membrane-bound PLC-δ enzymes for 1 nM PLC in the aqueous phase; see Appendix I).

Fig. 6 *A* shows the power spectrum of a bilayer-coated silica bead in a laser trap with an applied AC electric field that has a maximum value of 100 V/4.8 cm ≈ 20 V/cm.

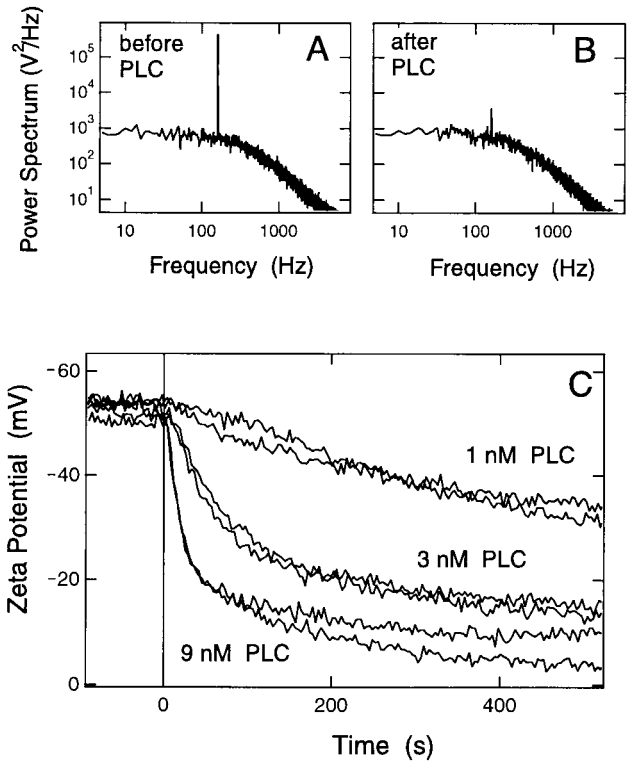

FIGURE 6 Effect of PLC-δ on the zeta potential of bilayer-coated silica beads as measured in the field/trap apparatus. The experimental approach is described in detail in Materials and Methods. Briefly, we used a tightly focused laser beam to trap a 500-nm-radius silica bead coated with a PC/PIP_2 bilayer (Fig. 1 *A*), then applied an AC electric field and monitored the displacement of the bead (Δx in Fig. 1 *A*) using a fast quadrant diode (Fig. 2). Using our calibrations of the stiffness of the trap and the sensitivity of the diode detector (Fig. 3 *A*), we calculated the net electrophoretic force on the coated bead (F_{el} in Fig. 1 *A*) from the displacement, Δx (Fig. 3 *B*). F_{el} is proportional to the zeta potential, ζ (Eq. 8), which is approximately proportional to the number of PIP_2 molecules on the outer leaflet coating the bead (Eq. 9). We follow the decline of ζ as a function of time as the bead is exposed to PLC-δ, which hydrolyzes the negatively charged lipid PIP_2 to produce the neutral lipid diacylglycerol (Fig. 1 *B*). (*A*) Power spectrum of a bead coated with PC/PIP_2, 2% PIP_2, when an AC field of 160 Hz is applied. The square root of the height of the peak at 160 Hz is proportional to the zeta potential. (*B*) Power spectrum of the same bead after exposure to 9 nM PLC-δ for 500 s. (*C*) Online measurements of the zeta potential of coated beads exposed to 1 nM, 3 nM, or 9 nM PLC-δ. The cross-channel containing the enzyme solution (Fig. 2) was opened at $t = 0$, allowing the solution to flow past the bead. The zeta potential was calculated from the height of the peak at 160 Hz from power spectra like those shown in *A* and *B*. Two beads coated with a PC/PIP_2 bilayer (2% PIP_2) were measured at each of the three PLC-δ concentrations.

Note the peak in the power spectrum at 160 Hz, which corresponds to the displacement of the bead in the field. The square root of the height of this peak is proportional to the net electrophoretic force exerted by the field on the bead. Thus, it is also proportional to the zeta potential (Eq. 8), which our field/trap measurements show is −55 mV (Fig. 6 *C*). To within a 20% approximation (see Eq. 9), the zeta potential is proportional to the fixed charge density on the

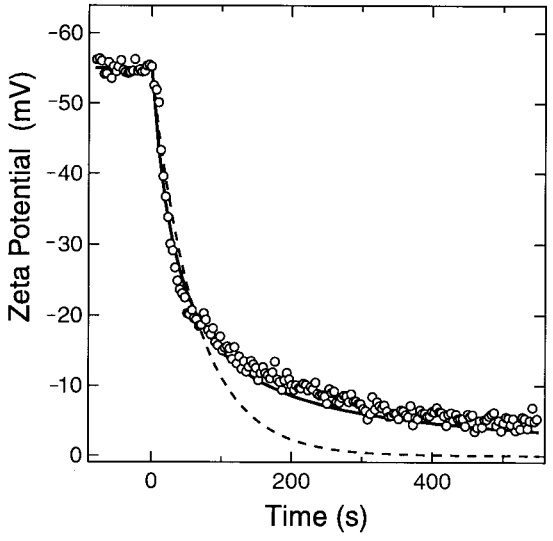

FIGURE 7 Enzyme kinetics measured on a single bilayer-coated silica bead. The zeta potentials (○) determined experimentally from one of the coated beads exposed to 9 nM PLC-δ (Fig. 6 *C*) are plotted as a function of time. An analysis using a single-exponential fit (— — —) does not describe the data well. An equation based on second-order kinetic theory (see Eq. 12) predicts that the zeta potential should decay as $\alpha/(c + kt)$, where α, c, and k are constants. This equation provides a better fit to the data (——).

outer monolayer coating the bead or to the number of PIP_2 molecules it contains, which in these experiments is 90,000 (assuming each lipid occupies 70 $Å^2$) before addition of PLC-δ.

Fig. 6 *B* shows the power spectrum of the coated bead after exposure to 9 nM PLC-δ for 500 s. The ~100-fold decrease in the peak at 160 Hz corresponds to an ~10-fold decrease in both the zeta potential (from −55 mV to ~−5 mV) and the number of PIP_2 molecules on the bead. Fig. 6 *C* illustrates experiments in which the field/trap apparatus was used to follow the zeta potential as a function of time after exposing the trapped bead to the solution containing PLC-δ (1, 3, or 9 nM); results obtained with two different beads at each concentration are shown to illustrate the reproducibility of the measurements. Before opening the cross-channel containing the PLC-δ solution ($t < 0$ s), the zeta potential is constant as a function of time. Once the cross-channel was opened ($t = 0$), we obtained a zeta potential measurement every 3 s (average of three power spectra); these data are connected by the continuous lines in Fig. 6 *C*. Our interpretation of the results shown in Fig. 6 *C* is that PLC-δ produces a marked, concentration-dependent decrease in the zeta potential by hydrolyzing the negatively charged lipid PIP_2 and producing the neutral lipid diacylglycerol (Fig. 1 *B*).

Several control experiments support this interpretation. First, if we omit PLC-δ from fluid flowing in the cross-channel, the zeta potential remains constant (within ~3 mV) for thousands of seconds (data not shown). Second, altering the flow velocity of fluid in the cross-channel does not affect the displacement of the coated bead produced by the electric field. (Cross-channel fluid flow does cause a measurable displacement of the bead in the trap perpendicular to the applied field, but this does not affect our measurements.) Third, the rate of hydrolysis produced by 3 nM PLC-δ decreases ~10-fold when the free $[Ca^{2+}]$ is decreased ~10-fold (from ~0.5 μM to ~0.05 μM), as expected for this calcium-dependent enzyme. Additional control experiments showed that 2 mM dithiothreitol, added to the cross-channel solution to prevent deterioration of the enzyme, did not affect the zeta potential of the coated beads, as expected for a neutral molecule. Fourth, we also measured the zeta potential in the conventional manner, determining the velocity of each bead shown in Fig. 6 *C* in a DC electric field at the beginning and end of the experiment, and the results always agreed with the zeta potential determined from the field/trap measurements. Furthermore, the initial zeta potential of a coated bead measured in our field/trap apparatus (−55 mV, Fig. 6 *C*) agreed with the zeta potential of multilamellar vesicles measured in a conventional microelectrophoresis apparatus (−56 mV, Fig. 5), which controls for a number of potential artifacts.

Control experiments also show that the action of PLC-δ does not depend strongly on the ionic strength of the solution: the rate of PLC-catalyzed hydrolysis of PIP_2, determined in conventional radioactive assays, is similar in solutions of 100, 10, and 1 mM ionic strength (data not shown). Thus we can extrapolate results shown in Fig. 6, which were obtained in a 10 mM HEPES solution (~3 mM ionic strength), to more physiological salt concentrations.

Kinetics of PLC-δ

What do we learn from these measurements? Fig. 7 shows the progress curve (changes in zeta potential or percent PIP_2 hydrolyzed versus time) for one of the beads exposed to 9 nM PLC-δ. Note that the decay cannot be described by a single-exponential function (dashed line); this is also true for the data obtained using 3 nM PLC-δ. A simple theory (Appendix II) takes into account previous structural and kinetic work showing that the enzyme requires two PIP_2 molecules: one binds to the PH domain of PLC-δ, attaching the enzyme to the surface (high-affinity binding), and the second interacts with the catalytic domain and is hydrolyzed (weak-affinity binding). In this dual-substrate model, the initial rate of hydrolysis should depend on the square of the surface concentration of PIP_2 (at least for low $[PIP_2]$), and the data in the literature are consistent with this model (Cifuentes et al., 1993; Wang et al., 1996; Bromann et al., 1997). The progress curve for such an enzyme should not be a single exponential but should decay with time as $1/(c + kt)$ (Appendix II). This expression (Fig. 7, solid line) does

describe our data better than a single exponential (Fig. 7, dashed line).

PLC-induced PIP_2 hydrolysis is proportional to [PLC]

Fig. 8 shows how the initial slopes of the curves in Fig. 6 *C* depend on the concentration of PLC-δ. The data can be described by a linear function, as expected from the known structure of the enzyme, the expectation that PLC-δ acts as a monomer, and previous work. The average of the slope from 15 experiments is ~ -0.1 mV/s per nM PLC-δ, close to the value shown in Fig. 8. Using this number and estimating the number of bound PLC-δ molecules, we can calculate the rate at which a single membrane-bound PLC-δ hydrolyzes PIP_2. Specifically, in a 1 nM PLC-δ solution, we estimate ~100 PLC-δ molecules bind initially to the surface of the coated bead, and the measured decline in the zeta potential of 0.1 mV/s implies hydrolysis of ~200 PIP_2/s ($\zeta \approx -50$ mV corresponds to $\sim 10^5$ PIP_2 molecules). Thus, a membrane-bound PLC-δ catalyzes hydrolysis of ~1 PIP_2/s under our conditions (0.5 μM free calcium). This calculation agrees well with published measurements using unsupported phospholipid bilayer vesicles or monolayers under comparable conditions (for reviews see Singer et al., 1997; Katan and Williams, 1997; Rhee et al., 2000). We are encouraged that our results, to our knowledge, the first reported use of supported membranes to study phosphoinositide-specific phospholipases, agree with the studies of this well characterized enzyme using the better established unsupported vesicle, monolayer, and micelle model systems.

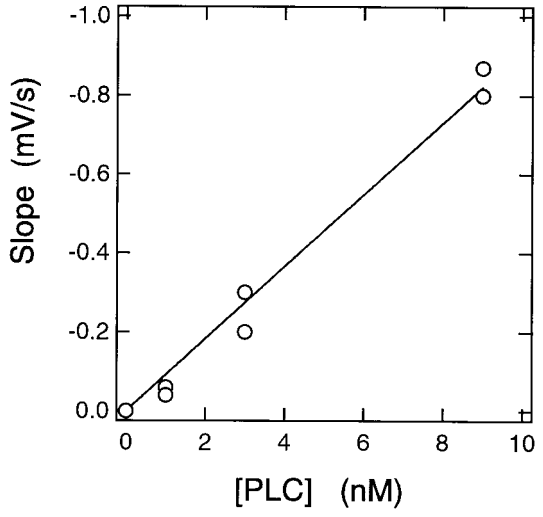

FIGURE 8 Relationship between the initial slope of the kinetic curves and enzyme concentration. As expected theoretically, the initial slopes of the kinetic curves (○), determined by fitting Eq. 12 to the data in Fig. 6 *C*, are proportional to the [PLC]. The straight line is the least-squares best fit to the data. Analysis of data from these and other similar experiments (not shown) gives an average slope ~ -0.1 mV/s per nM PLC.

DISCUSSION

This report focuses on describing the field/trap apparatus and demonstrating that it can provide useful information about a well-studied enzyme, PLC-δ. Fig. 6 shows that the apparatus can be used to follow the PLC-catalyzed hydrolysis of PIP_2 on a single bilayer-coated silica bead. The initial rate of hydrolysis is proportional to the [PLC] (Fig. 8), as expected from previous work. Reducing the free concentration of Ca^{2+} 10-fold decreases the initial rate of hydrolysis ~10-fold, an important control measurement for this calcium-dependent enzyme. The rate at which PLC-δ catalyzes hydrolysis of PIP_2 on bilayer-coated beads is similar to the rate obtained using vesicles and monolayers. Finally, the progress curve for PLC (Fig. 7) is not a single exponential, but decays with time as $1/(c + kt)$, as expected for an enzyme with second-order kinetics (see Appendix II).

Advantages of the field/trap apparatus

What are the advantages of the field/trap apparatus over conventional methods used to study enzyme kinetics? First, measurements can be made rapidly: the zeta potential measurements illustrated in Fig. 7 were obtained online every 3 s from an average of three power spectra. A related advantage is the system allows rapid mixing, with a dead time of ~1 s. Second, the measurements are accurate and reproducible, as illustrated by the data in Figs. 4 and 6 *C*, and allow us to determine how the fraction of PIP_2 in the membrane changes with time (Fig. 7). Third, measurements are made with a single bilayer. This was particularly important for PLC-δ because factors such as a possible slow exchange of enzyme between vesicles have confounded previous attempts to obtain progress curves for this enzyme. Fourth, the system allows continuous flow of the PLC-δ solution past the coated bead, replenishing any PLC-δ lost onto the walls of the chamber and carrying away the hydrolysis product IP_3, which inhibits the enzyme. The flux of IP_3 through the ~1-μm Nernstian unstirred layer is rapid. Fifth, the field/trap system can measure activity using unlabeled enzyme and substrate. In contrast, conventional enzymology measurements require radioactive, fluorescent, or other labels for detection. Sixth, and most importantly, the field/trap apparatus we describe might be refined to allow single-molecule enzymology measurements.

Comparison of supported versus conventional bilayers

We used bilayer-coated silica beads for the field/trap experiments for two reasons: first, the laser trap works efficiently

with the coated beads due to the high refractive index difference; second, the radius of the bead is known, which facilitates analysis of the data. The question arises, however, of whether PLC-δ activity on a glass-supported bilayer is comparable to activity seen on other model systems such as phospholipid vesicles or monolayers. We know of no other published data measuring lipase activity on a glass-supported bilayer membrane. SUVs have been used to form a single continuous membrane on planar glass surfaces (Brian and McConnell, 1984); Bayerl and Bloom (1990) pioneered the use of bilayer-coated silica beads for NMR studies. The bilayer deposited on silica beads is fluid (Köchy and Bayerl, 1993), and it is assumed to close up on a silica bead because phospholipids were found to completely wet the glass surfaces (Nissen et al., 1999). Nevertheless, the silica substrate could induce artifacts due to submicroscopic defects, lateral tension, asymmetry, or enhanced flip-flop rates in the supported bilayers. Although more work is required to validate the use of supported membranes in the study of enzyme kinetics, our results are encouraging because the kinetics of PLC-δ on a supported bilayer are comparable to those observed in a free vesicle system.

Single-molecule enzyme measurements?

There are several ways (e.g., reducing n, the number of PIP_2 molecules on the bead; increasing the enzyme's turnover number; or increasing the applied field) the field trap apparatus might be refined so that a single membrane-bound PLC-δ could be observed hydrolyzing most of the PIP_2 on a bead in a reasonable time ($<10^3$ s). Single-molecule studies of other enzymes have provided a deeper understanding of the kinetic mechanisms that underlie their behavior. Xie and Lu (1999) reviewed how a subtle analysis of single-molecule fluorescence measurements with cholesterol oxidase revealed dynamic disorder, i.e., slow conformational motions that influence enzyme function. Edman and Rigler (2000) consider the memory landscapes of single-enzyme molecules. PLCs are complicated enzymes with PH, EF hand, and C2 as well as catalytic domains. Like cholesterol oxidase, they may well exhibit slow conformational alterations at the membrane interface that affect enzyme activity. If so, the field/trap apparatus might detect these changes.

Kinetic measurements with single PLC-δ molecules could be confounded by the rapid adsorption/desorption of the enzyme from individual PIP_2 binding sites on coated beads. The PH domain of PLC-δ dissociates from PIP_2 with an off constant of ~10/s, equating to a lifetime of ~0.1 s (Hirose et al., 1999). Assuming the lifetime of the intact PLC-δ is similar, a rate of 10/s implies the enzyme will hydrolyze, on average, only one PIP_2 before desorbing. Thus, the conventional picture that PLC-δ remains bound to the surface through its PH domain, and scoots along the surface hydrolyzing many PIP_2 molecules (e.g., Cifuentes et al., 1993; Yagisawa et al., 1998), may require a slight revision. Berg (1983) in his analysis of diffusion adjacent to a surface noted that when a molecule diffuses a distance x from the surface of a sphere of radius r, it will revisit the sphere an average of r/x times before wandering away permanently (see also Goldstein and Dembo, 1995; Lagerholm and Thompson, 1998). Thus, when PLC-δ desorbs from one PIP_2 and moves 1 nm from the surface of a 500-nm-radius sphere, it will revisit the sphere ~500 times, where it is likely to encounter and adsorb to another PIP_2 and hydrolyze more lipid before random walking away for good. A similar phenomenon probably occurs at the plasma membrane. The ability to readily modify and express enzymes such as PLC-δ, combined with knowledge of their structure, should allow investigators to modify PLC-δ to attach it to a membrane more strongly. In principle, one could then dissect out the kinetics of adsorption/desorption phenomena from any interesting conformational changes.

Other uses for the field/trap apparatus

We envision other potential uses for the field/trap apparatus. For example, it could be used to study the activation of PLC-β by a G protein on a membrane (Rhee et al., 2000), the action of a phosphatidylinositol 3-kinase to form a more negatively charged phosphoinositide (Stephens et al., 2000; Rameh and Cantley, 1999), or the phospholipase D-catalyzed hydrolysis of zwitterionic PC to form negatively charged phosphatidic acid (Sciorra et al., 2000). These enzymes all change the charge of a membrane-bound substrate. More generally, any biophysical process that changes the surface charge of a bead can be followed. For example, the field/trap apparatus could be used to study adsorption of polyelectrolytes to membranes or glass. Finally, it may prove useful to study fundamental phenomena in colloid chemistry, such as relaxation of the double layer. Palberg et al. (1999) have already combined laser trapping and electrophoresis to investigate the electrokinetic colloidal properties of polystyrene spheres. In this context, the bilayer-coated silica beads used in our study might also be an appropriate model system for colloid studies, because, in contrast to the latex or polystyrene spheres that are often used (e.g., Russel et al., 1989), the surface of a bilayer-coated silica bead is smooth and the charge density is well defined.

APPENDIX I

Binding of PLC-δ to PC/PIP_2 bilayers

We need to know the association constant, K (assuming a 1:1 complex), between PLC-δ and PIP_2 when the phosphoinositide is present in a PC/PIP_2 bilayer to calculate how many enzyme molecules are bound to a bilayer-coated bead. Rebecchi et al. (1992) reported $K = 4 \times 10^5\ M^{-1}$ using PC/PIP_2 (2% PIP_2) vesicles, and Cifuentes et al. (1993) determined a value of $K = 7 \times 10^5\ M^{-1}$ for vesicles with the same PC/PIP_2 composition.

These numbers straddle the value of $K \approx 5 \times 10^5\ M^{-1}$ that can be deduced from data reported by Wang et al. (1996) for PC/PE/PIP_2 vesicles containing 4% PIP_2. The average of these three estimates is $K \approx 5 \times 10^5\ M^{-1}$. These measurements were made in solutions of ~100 mM ionic strength: the binding may be stronger in our 10 mM Hepes (~3 mM ionic strength) solutions. For the order of magnitude calculations that we wish to make in this paper, we assume that $K = 10^6\ M^{-1}$. Thus, when a solution containing 1 nM PLC-δ flows past the trapped bead, ~100 PLC-δ molecules adsorb to its surface ($K \times$ [PLC-δ] $\times\ n \approx 100$).

The 1:1 association constant reported for the isolated PH domain of PLC-δ with PIP_2 in a PC/PIP_2 vesicle is similar to that measured with the intact protein: Lemmon et al. (1995) reported $K = 5 \times 10^5\ M^{-1}$ for PC/PIP_2 (5% PIP_2) vesicles using titration calorimetry, as did Hirose et al. (1999) using PC/PIP_2 (3% PIP_2) vesicles adsorbed to a BIAcore sensor chip. Although the binding of the PH domain to PIP_2 is important for the function of the enzyme (Yagisawa et al., 1998), we do not wish to imply that the PH domain alone determines the binding of PLC-δ to membranes; the catalytic domain should contribute some binding energy. Furthermore, recent work suggests that both the C2 (Lomasney et al., 1999) and EF hand (Yamamoto et al., 1999) domains may also contribute to the membrane binding in a calcium-dependent manner.

APPENDIX II

Kinetics of PLC-δ-induced hydrolysis of PIP_2

For a conventional enzyme, the rate of hydrolysis of a substrate, S, is proportional to the substrate concentration, $d[S]/dt = -a[S]$, where a is a constant. Thus, the progress curve (substrate concentration versus time) is a single exponential.

For PLC-δ the substrate is membrane-bound PIP_2. It is the membrane-bound form of PLC-δ that hydrolyzes PIP_2 (Fig. 1), and the binding of the noncatalytic PH domain to PIP_2 provides the major contribution to the binding energy (Appendix I). Thus, the rate of hydrolysis of PIP_2 should be proportional to the square of the surface concentration of PIP_2 in the membrane, $[PIP_2]$: $d[PIP_2]/dt = -k[PIP_2]^2$, where k is a constant. As discussed for second-order rate equations in standard texts (Voet and Voet, 1995) the solution to this equation is $[PIP_2] = 1/(c + kt)$, where c is a constant equal to the reciprocal of the initial $[PIP_2]$ on the bead. The zeta potential, ζ, is approximately proportional to the surface concentration of PIP_2 (see Eq. 9), so the decay of ζ for a bilayer-coated silica bead, monitored as a function of time in our field/trap apparatus, should have the same form. Specifically, if we use the approximation that $\sinh x = x$ from Eq. 9, $\zeta = \alpha[PIP_2]$, where α is a constant given by Eq. 9. Thus:

$$\zeta = \frac{\alpha}{c + kt}. \tag{12}$$

We compared the predictions of this equation to the data we obtained from field/trap experiments (solid curve in Fig. 7): it describes the kinetics of PLC-δ more accurately than a single exponential (dashed curve in Fig. 7).

There are, however, three simplifications to our analysis of the zeta potential data using Eq. 12. First, ζ is proportional to the surface charge density, σ, or number of PIP_2 molecules on the bead, only when the potential is low; the Gouy equation, Eq. 9, gives the more exact relation. The maximum error introduced by assuming $\sinh x = x$ in Eq. 9 is ~20% for $x = 1$ or a zeta potential of −55 mV. Second, as hydrolysis proceeds and the zeta potential decreases (Fig. 6 *C*), the equilibrium association constant of the PH domain of PLC-δ and PIP_2 might decrease; thus, k in Eq. 12 might decrease with time. Third, as the zeta potential decreases, the local concentration of calcium in the diffuse double layer adjacent to the membrane will also decrease (Boltzmann factor), which may affect the activity of the enzyme. We ignore these complications in our kinetic analysis of the data. Additional work must be done to establish conclusively that the kinetics of PLC-δ are described better by Eq. 12 than by a single exponential.

We are grateful for helpful discussions with E.-L. Florin and C. Schmidt. We thank S. Pentyala and E. Tall for expression and purification of the recombinant human PLC-δ_1, G. Hangyás-Mihályné for excellent technical assistance with the steady-state microelectrophoresis measurements, and A. Morris for a generous gift of PIP_2.

This work was supported by grants Ra655/2–1 and SFB266-C14 from the German Science Foundation to J.R., by grant GM24971 from the National Institutes of Health and grant MCB9729538 from the National Science Foundation to S.M., and by grant GM43422 from the National Institutes of Health to M.R.

REFERENCES

Allersma, M. W., F. Gittes, M. J. deCastro, R. J. Stewart, and C. F. Schmidt. 1998. Two-dimensional tracking of ncd motility by back focal plane interferometry. *Biophys. J.* 74:1074–1085.

Ashkin, A. 1997. Optical trapping and manipulation of neutral particles using lasers. *Proc. Natl. Acad. Sci. U.S.A.* 94:4853–4860.

Bangham, A. D., R. Flemans, D. H. Heard, and G. V. F. Seaman. 1958. An apparatus for microelectrophoresis of small particles. *Nature.* 182: 642–644.

Barenholz, Y., D. Gibbes, B. J. Litman, J. Goll, T. E. Thompson, and R. D. Carlson. 1977. A simple method for the preparation of homogeneous phospholipid vesicles. *Biochemistry.* 16:2806–2810.

Bayerl, T. M., and M. Bloom. 1990. Physical properties of single phospholipid bilayers adsorbed to micro glass beads: a new vesicular model system studied by ^{2}H-nuclear magnetic resonance. *Biophys. J.* 58: 357–362.

Berg, H. C. 1983. Random Walks in Biology. Princeton University Press, Princeton, NJ.

Berridge, M. J. 1993. Inositol trisphosphate and calcium signalling. *Nature.* 361:315–325.

Brian, A. A., and H. M. McConnell. 1984. Allogeneic stimulation of cytotoxic T cells by supported planar membranes. *Proc. Natl. Acad. Sci. U.S.A.* 81:6159–6163.

Bromann, P. A., E. E. Boetticher, and J. W. Lomasney. 1997. A single amino acid substitution in the pleckstrin homology domain of phospholipase C-δ_1 enhances the rate of substrate hydrolysis. *J. Biol. Chem.* 272:16240–16246.

Cifuentes, M. E., L. Honkanen, and M. J. Rebecchi. 1993. Proteolytic fragments of phosphoinositide-specific phospholipase C-δ_1. Catalytic and membrane binding properties. *J. Biol. Chem.* 268:11586–11593.

Clapham, D. E. 1995. Calcium signaling. *Cell.* 80:259–268.

Edman, L., and R. Rigler. 2000. Memory landscapes of single-enzyme molecules. *Proc. Natl. Acad. Sci. U.S.A.* 97:8266–8271.

Essen, L. O., O. Perisic, R. Cheung, M. Katan, and R. L. Williams. 1996. Crystal structure of a mammalian phosphoinositide-specific phospholipase C-δ. *Nature.* 380:595–602.

Essen, L. O., O. Perisic, M. Katan, Y. Wu, M. F. Roberts, and R. L. Williams. 1997. Structural mapping of the catalytic mechanism for a mammalian phosphoinositide-specific phospholipase C. *Biochemistry.* 36:1704–1718.

Ferguson, K. M., M. A. Lemmon, J. Schlessinger, and P. B. Sigler. 1995. Structure of the high affinity complex of inositol trisphosphate with a phospholipase C pleckstrin homology domain. *Cell.* 83:1037–1046.

Florin, E.-L., A. Pralle, E. H. K. Stelzer, and J. K. H. Hörber. 1998. Photonic force microscope calibration by thermal noise analysis. *Appl. Phys. A.* 66:S75–S78.

Gittes, F., and C. F. Schmidt. 1998. Signals and noise in micromechanical measurements. *Methods Cell Biol.* 55:129–156.

Goldstein, B., and M. Dembo. 1995. Approximating the effects of diffusion on reversible reactions at the cell surface: ligand-receptor kinetics. *Biophys. J.* 68:1222–1230.

Grobler, J. A., L. Essen, R. L. Williams, and J. H. Hurley. 1996. C2 domain conformational changes in phospholipase C-δ_1. *Nat. Struct. Biol.* 3:788–795.

Groves, J. T., and S. G. Boxer. 1995. Electric field-induced concentration gradients in planar supported bilayers. *Biophys. J.* 69:1972–1975.

Groves, J. T., N. Ulman, P. S. Cremer, and S. G. Boxer. 1998. Substrate-membrane interactions: mechanisms for imposing patterns on a fluid bilayer membrane. *Langmuir.* 14:3347–3350.

Hirose, K., S. Kadowaki, M. Tanabe, H. Takeshiba, and M. Iino. 1999. Spatiotemporal dynamics of inositol 1,4,5-trisphosphate that underlies complex Ca^{2+} mobilization patterns. *Science.* 284:1527–1531.

Hondal, R. J., Z. Zhao, A. V. Kravchuk, H. Liao, S. R. Riddle, X. Yue, K. S. Bruzik, and M. D. Tsai. 1998. Mechanism of phosphatidylinositol-specific phospholipase C: a unified view of the mechanism of catalysis. *Biochemistry.* 37:4568–4580.

Hunter, R. J. 1981. Zeta Potential in Colloid Science. Academic Press, New York.

Hurley, J. H., and J. A. Grobler. 1997. Protein kinase C and phospholipase C: bilayer interactions and regulation. *Curr. Opin. Struct. Biol.* 7:557–565.

Hurley, J. H., and S. Misra. 2000. Signaling and subcellular targeting by membrane binding domains. *Annu. Rev. Biophys. Biomol. Struct.* 29: 49–79.

Katan, M., and R. L. Williams. 1997. Phosphoinositide-specific phospholipase C: structural basis for catalysis and regulatory interactions. *Semin. Cell. Dev. Biol.* 8:287–296.

Köchy, T., and T. M. Bayerl. 1993. Lateral diffusion coefficients of phospholipids in spherical bilayers on a solid support measured by ^{2}H-nuclear-magnetic-resonance relaxation. *Phys. Rev. E.* 47:2109–2116.

Lagerholm, B. C., and N. L. Thompson. 1998. Theory for ligand rebinding at cell membrane surfaces. *Biophys. J.* 74:1215–1228.

Lemmon, M. A., K. M. Ferguson, R. O'Brien, P. B. Sigler, and J. Schlessinger. 1995. Specific and high-affinity binding of inositol phosphates to an isolated pleckstrin homology domain. *Proc. Natl. Acad. Sci. U.S.A.* 92:10472–10476.

Lomasney, J. W., H. F. Cheng, S. R. Roffler, and K. King. 1999. Activation of phospholipase C-δ_1 through C2 domain by a Ca^{2+}-enzyme-phosphatidylserine ternary complex. *J. Biol. Chem.* 274:21995–22001.

McLaughlin, S. 1989. The electrostatic properties of membranes. *Annu. Rev. Biophys. Biophys. Chem.* 18:113–136.

Mehta, A. D., J. T. Finer, and J. A. Spudich. 1998. Reflections of a lucid dreamer: optical trap design considerations. *Methods Cell Biol.* 55: 47–69.

Millikan, R. A. 1917. The Electron: Its Isolation and Measurement and Determination of Some of Its Properties. The University of Chicago Press, Chicago.

Morris, A. J., S. A. Rudge, C. E. Mahlum, and J. M. Jenco. 1995. Regulation of phosphoinositide-3-kinase by G protein $\beta\gamma$ subunits in a rat osteosarcoma cell line. *Mol. Pharmacol.* 48:532–539.

Newton, A. C. 2000. Protein kinase C. *In* Principles of Molecular Regulation. P. M. Conn and A. R. Means, editors. Humana Press, Totowa, NJ. 207–220.

Nissen, J., S. Gritsch, G. Wiegand, and J. O. Rädler. 1999. Wetting of phospholipid membranes on hydrophilic surfaces: concepts towards self-healing membranes. *Eur. Phys. J. B.* 10:335–344.

O'Brien, R. W., and L. R. White. 1978. Electrophoretic mobility of a spherical colloidal particle. *J. Chem. Soc. Faraday II.* 74:1607–1626.

Overbeek, J. T., and P. H. Wiersema. 1967. The interpretation of electrophoretic mobilities. *In* Electrophoresis: Theory, Methods, and Applications. M. Bier, editor. Academic Press, New York. 1–50.

Palberg, T., M. Evers, N. Garbow, and D. Hessinger. 1999. Electrophoretic mobility of charged spheres. *In* Transport versus Structure in Biophysics and Chemistry. S. C. Mueller, J. Parisi, and W. Zimmermann, editors. Springer Verlag, Heidelberg, Germany. 191–213.

Rameh, L. E., and L. C. Cantley. 1999. The role of phosphoinositide 3-kinase lipid products in cell function. *J. Biol. Chem.* 274:8347–8350.

Rebecchi, M., A. Peterson, and S. McLaughlin. 1992. Phosphoinositide-specific phospholipase C-δ_1 binds with high affinity to phospholipid vesicles containing phosphatidylinositol 4,5-bisphosphate. *Biochemistry.* 31:12742–12747.

Rhee, S. G., B. Poulin, S. B. Lee, and F. Sekiya. 2000. Regulation of phosphoinositide-specific phospholipase C isozymes. *In* Biology of Phosphoinositides. S. Cockcroft, editor. Oxford University Press, Oxford, UK. 1–31.

Russel, W. B., D. A. Saville, and W. R. Schowalter. 1989. Colloidal Dispersions. The University Press, Cambridge, UK.

Sciorra, V. A., M. A. Frohman, and A. J. Morris. 2000. Regulation of phospholipase D signalling by phosphoinositides. *In* Biology of Phosphoinositides. S. Cockcroft, editor. Oxford University Press, Oxford, UK. 268–297.

Sheetz, M. P., editor. 1998. Laser Tweezers in Cell Biology. Academic Press, San Diego, CA.

Singer, W. D., H. A. Brown, and P. C. Sternweis. 1997. Regulation of eukaryotic phosphatidylinositol-specific phospholipase C and phospholipase D. *Annu. Rev. Biochem.* 66:475–509.

Stephens, L., A. McGregor, and P. Hawkins. 2000. Phosphoinositide 3-kinases: regulation by cell surface receptors and function of 3-phosphorylated lipids. *In* Biology of Phosphoinositides. S. Cockcroft, editor. Oxford University Press, Oxford, UK. 32–108.

Svoboda, K., and S. M. Block. 1994. Biological applications of optical forces. *Annu. Rev. Biophys. Biomol. Struct.* 23:247–285.

Tall, E., G. Dorman, P. Garcia, L. Runnels, S. Shah, J. Chen, A. Profit, Q. M. Gu, A. Chaudhary, G. D. Prestwich, and M. J. Rebecchi. 1997. Phosphoinositide binding specificity among phospholipase C isozymes as determined by photo-cross-linking to novel substrate and product analogs. *Biochemistry.* 36:7239–7248.

Toner, M., G. Vaio, A. McLaughlin, and S. McLaughlin. 1988. Adsorption of cations to phosphatidylinositol 4,5-bisphosphate. *Biochemistry.* 27: 7435–7443.

Voet, D., and J. G. Voet. 1995. Biochemistry. John Wiley and Sons, New York.

Wang, L. P., C. Lim, Y. Kuan, C. L. Chen, H. F. Chen, and K. King. 1996. Positive charge at position 549 is essential for phosphatidylinositol 4,5-bisphosphate-hydrolyzing but not phosphatidylinositol-hydrolyzing activities of human phospholipase C-δ_1. *J. Biol. Chem.* 271: 24505–24516.

Xie, X. S., and H. P. Lu. 1999. Single-molecule enzymology. *J. Biol. Chem.* 274:15967–15970.

Yagisawa, H., K. Sakuma, H. F. Paterson, R. Cheung, V. Allen, H. Hirata, Y. Watanabe, M. Hirata, R. L. Williams, and M. Katan. 1998. Replacements of single basic amino acids in the pleckstrin homology domain of phospholipase C-δ_1 alter the ligand binding, phospholipase activity, and interaction with the plasma membrane. *J. Biol. Chem.* 273:417–424.

Yamamoto, T., H. Takeuchi, T. Kanematsu, V. Allen, H. Yagisawa, U. Kikkawa, Y. Watanabe, A. Nakasima, M. Katan, and M. Hirata. 1999. Involvement of EF hand motifs in the Ca^{2+}-dependent binding of the pleckstrin homology domain to phosphoinositides. *Eur. J. Biochem.* 265:481–490.